mywbut.com

2.3 Impulse voltages

The first kind are lightning overvoltages, originated by lightning strokes hitting the phase wires of overhead lines or the busbars of outdoor substations. The amplitudes are very high, usually in the order of 1000 kV or more, as every stroke may inject lightning currents up to about 100 kA and even more into the transmission line;[27] each stroke is then followed by travelling waves, whose amplitude is often limited by the maximum insulation strength of the overhead line. The rate of voltage rise of such a travelling wave is at its origin directly proportional to the steepness of the lightning current, which may exceed 100 kA/μsec, and the voltage levels may simply be calculated by the current multiplied by the effective surge impedance of the line. Too high voltage levels are immediately chopped by the breakdown of the insulation and therefore travelling waves with steep wave fronts and even steeper wave tails may stress the insulation of power transformers or other h.v. equipment severely. Lightning protection systems, surge arresters and the different kinds of losses will damp and distort the travelling waves, and therefore lightning overvoltages with very different waveshapes are present within the transmission system.

The second kind is caused by switching phenomena. Their amplitudes are always related to the operating voltage and the shape is influenced by the impedances of the system as well as by the switching conditions. The rate of voltage rise is usually slower, but it is well known that the waveshape can also be very dangerous to different insulation systems, especially to atmospheric air insulation in transmission systems with voltage levels higher than 245 kV.[28]

Both types of overvoltages are also effective in the l.v. distribution systems, where they are either produced by the usual, sometimes current-limiting, switches or where they have been transmitted from the h.v. distribution systems. Here they may often cause a breakdown of electronic equipment, as they can reach amplitudes of several kilovolts, and it should be mentioned that the testing of certain l.v. apparatus with transient voltages or currents is a need today.[29] Such tests also involve 'electromagnetic compatibility (EMC) tests', which will not be discussed here.

Although the actual shape of both kinds of overvoltages varies strongly, it became necessary to simulate these transient voltages by relatively simple means for testing purposes. The various national and international standards define the impulse voltages as a unidirectional voltage which rises more or less rapidly to a peak value and then decays relatively slowly to zero. In the relevant IEC Standard 60,[2] widely accepted today through national committees,[3] a distinction is made between lightning and switching impulses, i.e. according to the origin of the transients. Impulse voltages with front durations varying from less than one up to a few tens of microseconds are, in general, considered as lightning impulses. Figure 2.23(a) shows the shape for such a 'full' lightning impulse voltage as well as sketches for the same voltage chopped at the tail (Fig. 2.23(b)) or on the front (Fig. 2.23(c)), i.e. interrupted by a

mywbut.com

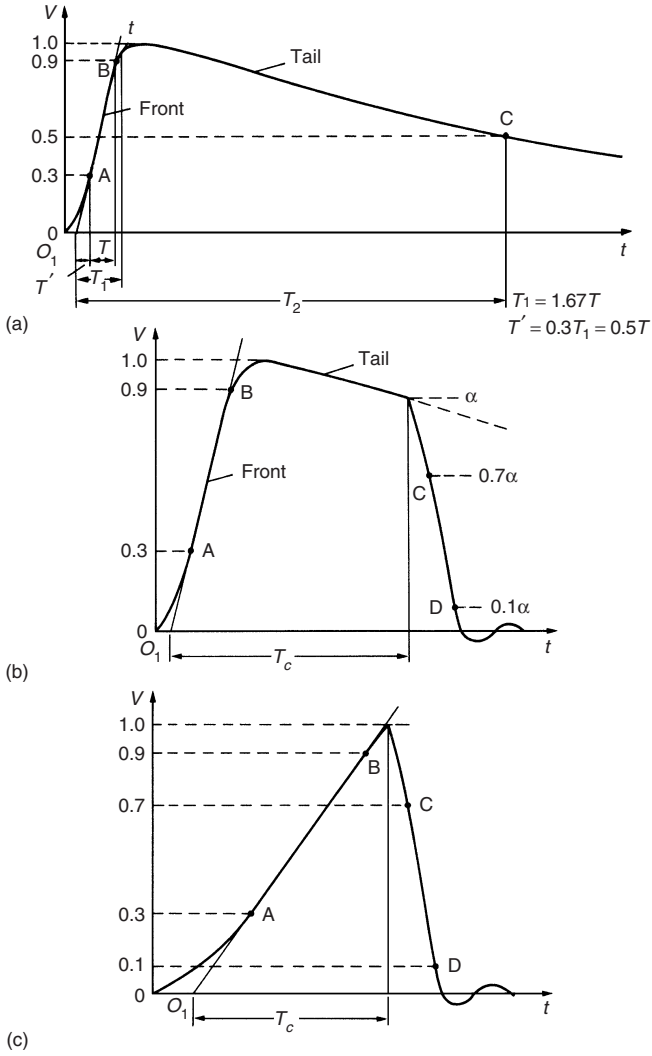


Figure 2.23 *General shape and definitions of lightning impulse (LI) voltages. (a) Full LI. (b) LI chopped on the tail. (c) LI chopped on the front. T_1: front time. T_2: time to half-value. T_c: time to chopping. O_1: virtual origin*

disruptive discharge. Although the definitions are clearly indicated, it should be emphasized that the 'virtual origin' O_1 is defined where the line AB cuts the time axis. The 'front time' T_1, again a virtual parameter, is defined as 1.67 times the interval T between the instants when the impulse is 30 per cent and 90 per cent of the peak value for full or chopped lightning impulses.

mywbut.com

For front-chopped impulses the 'time to chopping' T_c is about equal to T_1. The reason for defining the point A at 30 per cent voltage level can be found in most records of measured impulse voltages. It is quite difficult to obtain a smooth slope within the first voltage rise, as the measuring systems as well as stray capacitances and inductances may cause oscillations. For most applications, the (virtual) front time T_1 is 1.2 μs, and the (virtual) time to half-value T_2 is 50 μs. In general the specifications[2] permit a tolerance of up to ±30 per cent for T_1 and ±20 per cent for T_2. Such impulse voltages are referred to as a T_1/T_2 impulse, and therefore the 1.2/50 impulse is the accepted standard lightning impulse voltage today. Lightning impulses are therefore of very short duration, mainly if they are chopped on front. Due to inherent measurement errors (see Chapter 3, section 3.6) and uncertainties in the evaluation the 'time parameters' T_1, T_2 and T_c or especially the time difference between the points C and D (Figs 2.23(b) and (c)) can hardly be quantified with high accuracy.

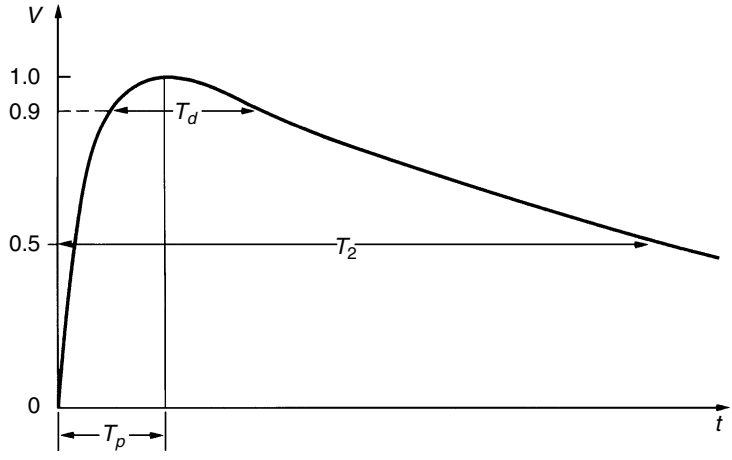


Figure 2.24 *General shape of switching impulse voltages. T_p: time to peak. T_2: time to half-value. T_d: time above 90 per cent*

Figure 2.24 illustrates the slope of a switching impulse. Whereas the time to half-value T_2 is defined similarly as before, the time to peak T_p is the time interval between the *actual* origin and the instant when the voltage has reached its maximum value. This definition could be criticized, as it is difficult to establish the actual crest value with high accuracy. An additional parameter is therefore the time T_d, the time at 90 per cent of crest value. The different definitions in comparison to lightning impulses can be understood if the time scale

mywbut.com

is emphasized: the standard switching impulse has time parameters (including tolerances) of

$$T_p = 250\,\mu s \pm 20\%$$

$$T_2 = 2500\,\mu s \pm 60\%$$

and is therefore described as a 250/2500 impulse. For fundamental investigations concerning the insulation strength of long air gaps or other apparatus, the time to peak has to be varied between about 100 and 1000 μs, as the breakdown strength of the insulation systems may be sensitive upon the voltage waveshape.[28]

2.3.1 Impulse voltage generator circuits

The introduction to the full impulse voltages as defined in the previous section leads to simple circuits for the generation of the necessary waveshapes. The rapid increase and slow decay can obviously be generated by discharging circuits with two energy storages, as the waveshape may well be composed by the superposition of two exponential functions. Again the load of the generators will be primarily capacitive, as insulation systems are tested. This load will therefore contribute to the stored energy. A second source of energy could be provided by an inductance or additional capacitor. For lightning impulses mainly, a fast discharge of pure inductor is usually impossible, as h.v. chokes with high energy content can never be built without appreciable stray capacitances. Thus a suitable fast discharge circuit will always consist essentially of two capacitors.

Single-stage generator circuits

Two basic circuits for single-stage impulse generators are shown in Fig. 2.25. The capacitor C_1 is slowly charged from a d.c. source until the spark gap G breaks down. This spark gap acts as a voltage-limiting and voltage-sensitive switch, whose ignition time (time to voltage breakdown) is very short in comparison to T_1. As such single-stage generators may be used for charging voltages from some kV up to about 1 MV, the sphere gaps (see Chapter 3, section 3.1) will offer proper operating conditions. An economic limit of the charging voltage V_0 is, however, a value of about 200 to 250 kV, as too large diameters of the spheres would otherwise be required to avoid excessive inhomogeneous field distributions between the spheres. The resistors R_1, R_2 and the capacitance C_2 form the waveshaping network. R_1 will primarily damp the circuit and control the front time T_1. R_2 will discharge the capacitors and therefore essentially control the wavetail. The capacitance C_2 represents the full load, i.e. the object under test as well as all other capacitive elements which are in parallel to the test object (measuring devices; additional load capacitor

mywbut.com

to avoid large variations of T_1/T_2, if the test objects are changed). No inductances are assumed so far, and are neglected in the first fundamental analysis, which is also necessary to understand multistage generators. In general this approximation is permissible, as the inductance of all circuit elements has to be kept as low as possible.

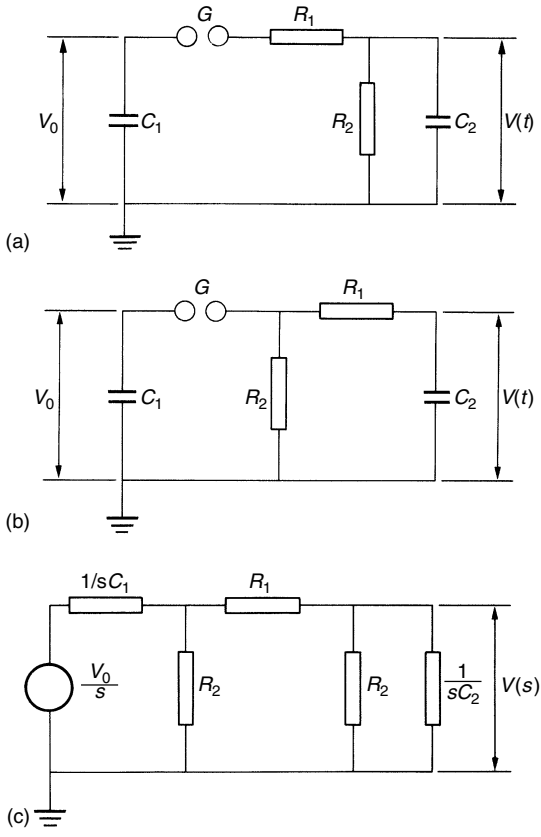


Figure 2.25 *Single-stage impulse generator circuits (a) and (b). C_1: discharge capacitance. C_2: load capacitance. R_1: front or damping resistance. R_2: discharge resistance. (c) Transform circuit*

Before starting the analysis, we should mention the most significant parameter of impulse generators. This is the maximum stored energy

$$W = \tfrac{1}{2} C_1 (V_{0_{\max}})^2 \tag{2.22}$$

within the 'discharge' capacitance C_1. As C_1 is always much larger than C_2, this figure determines mainly the cost of a generator.

mywbut.com

For the analysis we may use the Laplace transform circuit sketched in Fig. 2.25(c), which simulates the boundary condition, that for $t \leq 0$ C_1 is charged to V_0 and for $t > 0$ this capacitor is directly connected to the wave-shaping network. For the circuit Fig. 2.25(a) the output voltage is thus given by the expression

$$V(s) = \frac{V_0}{s} \frac{Z_2}{Z_1 + Z_2},$$

where

$$Z_1 = \frac{1}{C_1 s} + R_1;$$

$$Z_2 = \frac{R_2/C_2 s}{R_2 + 1/C_2 s}.$$

By substitution we find

$$V(s) = \frac{V_0}{k} \frac{1}{s^2 + as + b} \tag{2.23}$$

where

$$a = \left(\frac{1}{R_1 C_1} + \frac{1}{R_1 C_2} + \frac{1}{R_2 C_2} \right);$$

$$b = \left(\frac{1}{R_1 R_2 C_1 C_2} \right);$$

$$k = R_1 C_2. \tag{2.24}$$

For circuit Fig. 2.25(b) one finds the same general expression (eqn (2.23)), with the following constants; however,

$$\left.\begin{aligned} a &= \left(\frac{1}{R_1 C_1} + \frac{1}{R_1 C_2} + \frac{1}{R_2 C_1} \right); \\ b &= \left(\frac{1}{R_1 R_2 C_1 C_2} \right); \\ k &= R_1 C_2. \end{aligned}\right\} \text{ as above} \tag{2.25}$$

For both circuits, therefore, we obtain from the transform tables the same expression in the time domain:

$$V(t) = \frac{V_0}{k} \frac{1}{(\alpha_2 - \alpha_1)} [\exp(-\alpha_1 t) - \exp(-\alpha_2 t)] \tag{2.26}$$

mywbut.com

where α_1 and α_2 are the roots of the equation $s^2 + as + b = 0$, or

$$\alpha_1, \alpha_2 = \frac{a}{2} \mp \sqrt{\left(\frac{a}{2}\right)^2 - b}. \tag{2.27}$$

The output voltage $V(t)$ is therefore the superposition of two exponential functions of different signs. According to eqn (2.27), the negative root leads to a larger time constant $1/\alpha_1$ than the positive one, which is $1/\alpha_2$. A graph of the expression (eqn (2.26)) is shown in Fig. 2.26, and a comparison with Figs 2.23 and 2.24 demonstrates the possibility to generate both types of impulse voltages with these circuits.

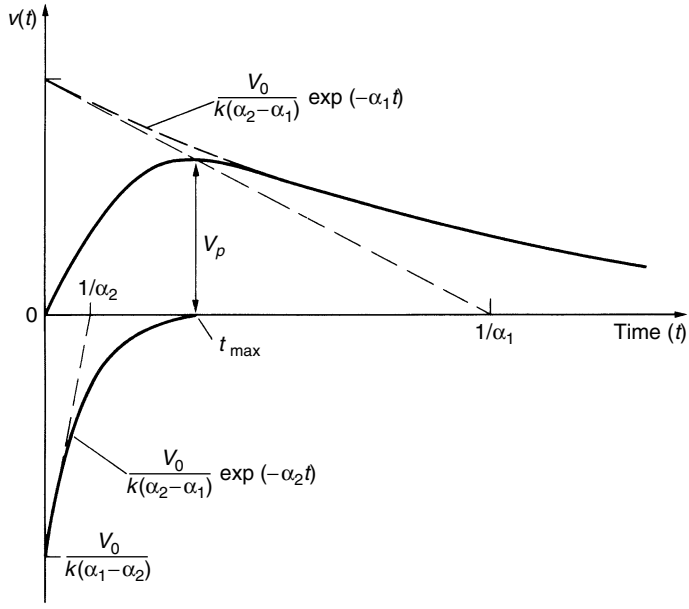


Figure 2.26 *The impulse voltage wave and its components according to circuits in Fig. 2.25*

Although one might assume that both circuits are equivalent, a larger difference may occur if the voltage efficiency, η, is calculated. This efficiency is defined as

$$\eta = \frac{V_p}{V_0}; \tag{2.28}$$

V_p being the peak value of the output voltage as indicated in Fig. 2.26. Obviously this value is always smaller than 1 or 100 per cent. It can be calculated

mywbut.com

by finding t_{max} from $dV(t)/dt = 0$; this time for the voltage $V(t)$ to rise to its peak value is given by

$$t_{max} = \frac{\ln(\alpha_2/\alpha_1)}{(\alpha_2 - \alpha_1)}. \tag{2.29}$$

Substituting this equation into eqn (2.26), one may find

$$\eta = \frac{(\alpha_2/\alpha_1)^{-[(\alpha_2/\alpha_1-\alpha_1)]} - (\alpha_2/\alpha_1)^{-[(\alpha_2/\alpha_2-\alpha_1)]}}{k(\alpha_2 - \alpha_1)}. \tag{2.30}$$

For a given impulse shape T_1/T_2 or T_p/T_2 of the impulse voltages the values of α_1 and α_2 must be equal. The differences in efficiency η can only be due, therefore, to differences in the value of $k = R_1C_2$ for both circuits. We may first calculate this term for the circuit Fig. 2.25(b), which has always a higher efficiency for a given ratio of C_2/C_1, as during the discharge the resistors R_1 and R_2 do not form a voltage-dividing system. The product R_1C_2 is found by eqn (2.27) by forming

$$\begin{aligned} \alpha_1 \cdot \alpha_2 &= b \\ \alpha_1 + \alpha_2 &= a \end{aligned} \tag{2.31}$$

and by the substitution of a and b from eqn (2.25). Then we obtain

$$k = R_1C_2 = \frac{1}{2}\left(\frac{\alpha_2 + \alpha_1}{\alpha_2 \cdot \alpha_1}\right)\left[1 - \sqrt{1 - 4\frac{\alpha_2 \cdot \alpha_1}{(\alpha_2 + \alpha_1)^2}\left(1 + \frac{C_2}{C_1}\right)}\right]. \tag{2.32}$$

For $C_2 \leq C_1$, which is fulfilled in all practical circuits, and with $\alpha_2 \gg \alpha_1$ for all normalized waveshapes, one may simplify this equation to

$$k \cong \frac{1 + C_2/C_1}{(\alpha_2 + \alpha_1)}. \tag{2.33}$$

The substitution of this expression in eqn (2.30) finally results in

$$\eta = \frac{C_1}{(C_1 + C_2)} = \frac{1}{1 + (C_2/C_1)} \tag{2.34}$$

if again the inequality $\alpha_2 \gg \alpha_1$ is taken into account. The voltage efficiency for this circuit will therefore rise continuously, if (C_2/C_1) decreases to zero. Equation (2.34) indicates the reason why the discharge capacitance C_1 should be much larger than the load C_2.

Less favourable is the circuit Fig. 2.25(a). The calculation of η may be based upon the substitution of α_1 and α_2 in eqn (2.30) from eqn (2.27), and a treatment of the ratio $R_1/R_2 = f(C_2/C_1)$, which increases heavily with

mywbut.com

decreasing values of C_2/C_1. With minor approximations and the inequality $\alpha_2 \gg \alpha_1$ one may find the result

$$\eta \cong \frac{C_1}{(C_1 + C_2)} \frac{R_2}{(R_1 + R_2)} = \frac{1}{(1 + C_2/C_1)} \frac{1}{(1 + R_1/R_2)}. \tag{2.35}$$

The comparison with eqn (2.34) shows the decrease in η due to an additional factor. As the ratio R_1/R_2 is dependent upon the waveshape, the simple dependency from (C_2/C_1) only is lost. For a 1.2/50 µs impulse and similar impulse voltages the rapid increase of R_1/R_2 leads to a decrease of η for $C_2/C_1 \lessapprox 0.1$; therefore, the efficiency moves through an optimum value and decreases for high C_2/C_1 values as well as for small ones. One could even show that for very small C_2/C_1 ratios this circuit will fail to work.

In practice, both circuits are in use, often, however, in mixed and modified form. If resistive h.v. dividers are placed in parallel to the test object, their resistor value may contribute to discharge the circuits. The front resistor R_1 is often subdivided, mainly in multistage generators treated later on. Nevertheless, the dependency of the voltage efficiency factors η is displayed in Fig. 2.27 for the standard lightning impulse voltage 1.2/50 µsec as well as for some other waveshapes. More information is available in the literature.[30]

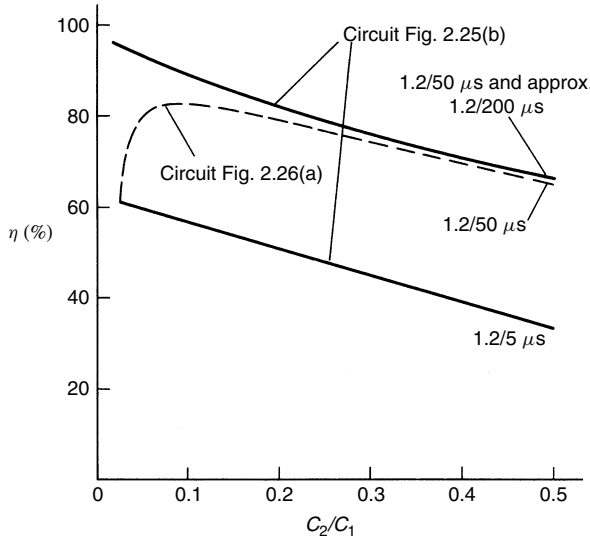


Figure 2.27 *Voltage efficiency factors η in dependency of the capacitance ratio C_2/C_1 for lightning impulses T_1/T_2*

Dimensioning of circuit elements. The common task is to find the resistor values for R_1 and R_2, as C_2 and C_1 are known in general. For larger

mywbut.com

generators, the discharge capacitors are always given and dimensioned for a good efficiency (see eqns (2.34) and (2.35)) within a certain range of C_2. This total load capacitance can easily be measured if it is not known in advance. The unknown resistance values can then be calculated using eqn (2.31) and the circuit-dependent values for a and b due to eqns (2.24) and (2.25). The result will be for:

Circuit Fig. 2.25(a):

$$R_1 = \frac{1}{2C_1}\left[\left(\frac{1}{\alpha_1}+\frac{1}{\alpha_2}\right) - \sqrt{\left(\frac{1}{\alpha_1}+\frac{1}{\alpha_2}\right)^2 - \frac{4(C_1+C_2)}{\alpha_1\alpha_2 \cdot C_2}}\right]. \tag{2.36}$$

$$R_2 = \frac{1}{2(C_1+C_2)}\left[\left(\frac{1}{\alpha_1}+\frac{1}{\alpha_2}\right) + \sqrt{\left(\frac{1}{\alpha_1}+\frac{1}{\alpha_2}\right)^2 - \frac{4(C_1+C_2)}{\alpha_1\alpha_2 C_2}}\right]. \tag{2.37}$$

Circuit Fig. 2.25(b):

$$R_1 = \frac{1}{2C_2}\left[\left(\frac{1}{\alpha_1}+\frac{1}{\alpha_2}\right) - \sqrt{\left(\frac{1}{\alpha_1}+\frac{1}{\alpha_2}\right)^2 - \frac{4(C_1+C_2)}{\alpha_1\alpha_2 C_1}}\right]. \tag{2.38}$$

$$R_2 = \frac{1}{2(C_1+C_2)}\left[\left(\frac{1}{\alpha_1}+\frac{1}{\alpha_2}\right) + \sqrt{\left(\frac{1}{\alpha_1}+\frac{1}{\alpha_2}\right)^2 - \frac{4(C_1+C_2)}{\alpha_1\alpha_2 C_1}}\right]. \tag{2.39}$$

All these equations contain the time constants $1/\alpha_1$ and $1/\alpha_2$, which depend upon the waveshape. There is, however, no simple relationship between these time constants and the times T_1, T_2 and T_p as defined in the national or international recommendations, i.e. in Figs 2.23 and 2.24. This relationship can be found by applying the definitions to the analytical expression for $V(t)$, this means to eqn (2.26). The relationship is irrational and must be computed numerically. The following table shows the result for some selected waveshapes:

T_1/T_2 (μs)	T_p/T_2 (μs)	$1/\alpha_1$ (μs)	$1/\alpha_2$ (μs)
1.2/5	–	3.48	0.80
1.2/50	–	68.2	0.405
1.2/200	–	284	0.381
250/2500	–	2877	104
–	250/2500	3155	62.5

mywbut.com

The standardized nominal values of T_1 and T_2 are difficult to achieve in practice, as even for fixed values of C_1 the load C_2 will vary and the exact values for R_1 and R_2 according to eqns (2.38) and (2.39) are in general not available. These resistors have to be dimensioned for the rated high voltage of the generator and are accordingly expensive. The permissible tolerances for T_1 and T_2 are therefore necessary and used to graduate the resistor values. A recording of the real output voltage $V(t)$ will in addition be necessary if the admissible impulse shape has to be testified.

Another reason for such a measurement is related to the value of the test voltage as defined in the recommendations.[2,3] This magnitude corresponds to the crest value, if the shape of the lightning impulse is smooth. However, oscillations or an overshoot may occur at the crest of the impulse. If the frequency of such oscillations is not less than 0.5 MHz or the duration of overshoot not over 1 μsec, a 'mean curve' (see Note below) should be drawn through the curve. The maximum amplitude of this 'mean curve' defines the value of the test voltage. Such a correction is only tolerated, provided their single peak amplitude is not larger than 5 per cent of the crest value. Oscillations on the front of the impulse (below 50 per cent of the crest value) are tolerated, provided their single peak amplitude does not exceed 25 per cent of the crest value. It should be emphasized that these tolerances constitute the permitted differences between specified values and those actually recorded by measurements. Due to measuring errors the true values and the recorded ones may be somewhat different.

Note. With the increasing application of transient or digital recorders in recording of impulse voltages it became very obvious that the definition of a 'mean curve' for the evaluation of lightning impulse parameters of waveforms with oscillations and/or overshoot, as provided by the standards,[2,3] is insufficient. Any software, written to evaluate the parameters, needs clear instructions which are not yet available. As this matter is still under consideration (by CIGRE Working Group 33.03) and a revision of the current standards may provide solutions, no further comments to this problem are given.

The origin of such oscillations or the overshoot can be found in measuring errors (heavily oscillating 'step response', see Chapter 3, section 3.6) as well as by the inductances within every branch of the circuit or the stray capacitances, which will increase with the physical dimensions of the circuit. As far as inductances are concerned, a general rule for the necessary critical damping of single-stage or – with less accuracy – of multistage generators can easily be demonstrated by Fig. 2.28. If individual inductances L_1, L_2 are considered within the discharge circuit as indicated in Fig. 2.28(a), a second order differential equation determines the output voltage across the load capacitance C_2. However, such an equivalent circuit cannot be exact, as additional circuits related to stray capacitances are not taken into account. Thus we may only

mywbut.com

combine the total inductance within the C_1-C_2 circuit to single inductance L, as shown in Fig. 2.28(b), and neglect the positions of the tail resistors, which have no big influence. This reduces the circuit to a simple damped series resonant circuit, and the critical resistance $R = R_1$ for the circuit to be non-oscillatory is given by the well-known equation

$$R_1 \cong R = 2\sqrt{\frac{L}{C}} \tag{2.40}$$

where

$$\frac{1}{C} = \frac{1}{C_1} + \frac{1}{C_2}$$

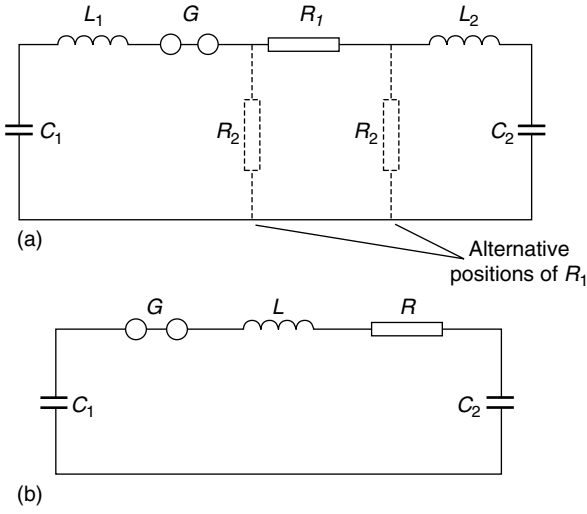


Figure 2.28 *Simplified circuit of impulse generator and load. Circuit showing alternative positions of the wave tail control resistance. (b) Circuit for calculation of wave front oscillations*

This equation is in general suitable for predicting the limiting values for the front resistor R_1. The extremely tedious analytical analysis of circuits containing individual inductances is shown elsewhere.[31–34] Computer programs for transients may also be used to find the origin of oscillations, although it is difficult to identify good equivalent circuits.

Multistage impulse generator circuits

The difficulties encountered with spark gaps for the switching of very high voltages, the increase of the physical size of the circuit elements, the efforts

mywbut.com

necessary in obtaining high d.c. voltages to charge C_1 and, last but not least, the difficulties of suppressing corona discharges from the structure and leads during the charging period make the one-stage circuit inconvenient for higher voltages.

In order to overcome these difficulties, in 1923 Marx[35] suggested an arrangement where a number of condensers are charged in parallel through high ohmic resistances and then discharged in series through spark gaps. There are many different, although always similar, multistage circuits in use. To demonstrate the principle of operation, a typical circuit is presented in Fig. 2.29 which shows the connections of a six-stage generator. The d.c. voltage charges the equal stage capacitors C_1' in parallel through the high value charging resistors R' as well as through the discharge (and also charging)

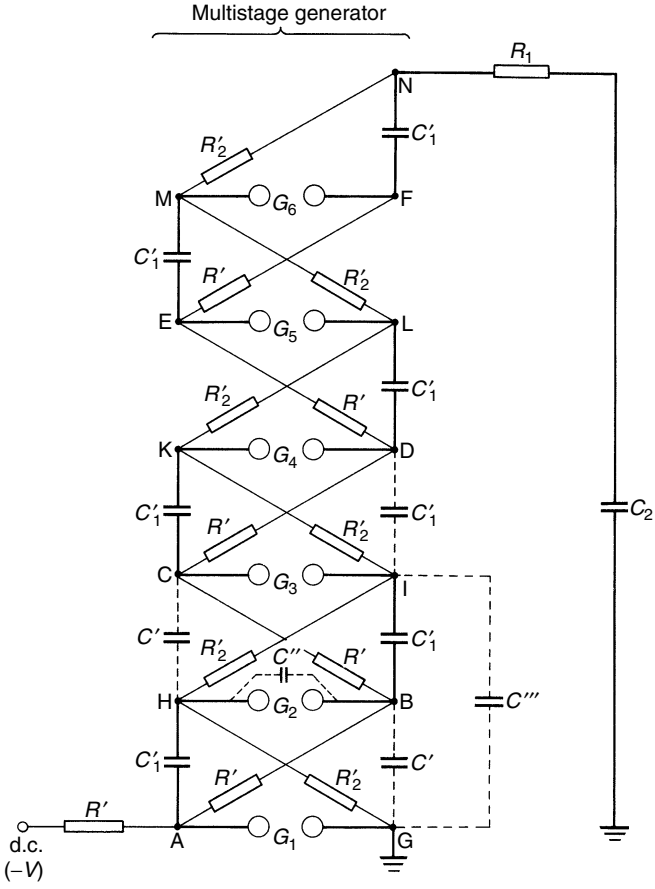


Figure 2.29 *Basic circuit of a six-stage impulse generator (Marx generator)*

mywbut.com

resistances R_2', which are much smaller than the resistors R' and are comparable with R_2 in Fig. 2.25. At the end of the relatively long charging period (typically several seconds up to 1 minute), the points $A, B, \ldots, F$ will be at the potential of the d.c. source, e.g. $-V$ with respect to earth, and the points $G, H, \ldots, N$ will remain at the earth potential, as the voltage drop during charging across the resistors R_2' is negligible. The discharge or firing of the generator is initiated by the breakdown of the lowest gap G_1 which is followed by a nearly simultaneous breakdown of all the remaining gaps. According to the traditional theory, which does not take into account the stray capacitances indicated by the dotted lines, this rapid breakdown would be caused by high overvoltages across the second and further gaps: when the first gap fires, the potential at point A changes rapidly from $-V$ to zero, and thus the point H increases its potential to $+V$. As the point B still would remain at the charging potential, $-V$, thus a voltage of $2V$ would appear across G_2. This high overvoltage would therefore cause this gap to break down and the potential at point I would rise to $+2V$, creating a potential difference of $3V$ across gap G_3, if again the potential at point C would remain at the charging potential. This traditional interpretation, however, is wrong, since the potentials B and C can – neglecting stray capacitances – also follow the adjacent potentials of the points A and B, as the resistors R' are between. We may only see up to now that this circuit will give an output voltage with a polarity opposite to that of the charging voltage.

In practice, it has been noted that the gap G_2 must be set to a gap distance only slightly greater than that at which G_1 breaks down; otherwise it does not operate. According to Edwards, Husbands and Perry[31] for an adequate explanation one may assume the stray capacitances C', C'' and C''' within the circuit. The capacitances C' are formed by the electrical field between adjacent stages; C''' has a similar meaning across two stages. C'' is the capacitance of the spark gaps. If we assume now the resistors as open circuits, we may easily see that the potential at point B is more or less fixed by the relative magnitudes of the stray capacitances. Neglecting C' between the points H and C and taking into account that the discharge capacitors C_1' are large in comparison to the stray capacitances, point B can be assumed as mid-point of a capacitor voltage divider formed by C'' and C'/C'''. Thus the voltage rise of point A from $-V$ to zero will cause the potential B to rise from $-V$ to a voltage of

$$V_B = -V + V\left(\frac{C''}{C' + C'' + C'''}\right) = -V\left(\frac{C' + C'''}{C' + C'' + C'''}\right).$$

Hence the potential difference across G_2 becomes

$$V_{G2} = +V - (-V_B) = V\left(1 + \frac{C' + C'''}{C' + C'' + C'''}\right).$$

mywbut.com

If C'' equals zero, the voltage across G_2 will reach its maximum value $2\,V$. This gap capacitance, however, cannot be avoided. If the stage capacitances C' and C''' are both zero, V_{G2} will equal V, and a sparking of G_2 would not be possible. It is apparent, therefore, that these stray capacitances enhance favourable conditions for the operation of the generator. In reality, the conditions set by the above equations are approximate only and are, of course, transient, as the stray capacitances start to discharge via the resistors. As the values of C' to C''' are normally in the order of some 10 pF only, the time constants for this discharge may be as low as 10^{-7} to 10^{-8} sec.

Thus the voltage across G_2 appears for a short time and leads to breakdown within several tens of nanoseconds. Transient overvoltages appear across the further gaps, enhanced also by the fact that the output terminal N remains at zero potential mainly, and therefore additional voltages are built up across the resistor R'_2. So the breakdown continues and finally the terminal N attains a voltage of $+6V$, or nV, if n stages are present.

The processes associated with the firing of such generators are even more sophisticated. They have been thoroughly analysed and investigated experimentally.[31,36,37]

In practice for a consistent operation it is necessary to set the distance for the first gap G_1 only slightly below the second and further gaps for earliest breakdown. It is also necessary to have the axes of the gaps in one vertical plane so that the ultraviolet illumination from the spark in the first gap irradiates the other gaps. This ensures a supply of electrons released from the gap to initiate breakdown during the short period when the gaps are subjected to the overvoltage. If the first gap is not electronically triggered, the consistency of its firing and stability of breakdown and therefore output voltage is improved by providing ultraviolet illumination for the first gap. These remarks indicate only a small part of the problems involved with the construction of spark gaps and the layout of the generator. Before some of these additional problems are treated, we shall treat more realistic Marx circuits as used for the explanations so far.

In Fig. 2.29, the wavefront control resistor R_1 is placed between the generator and the load only. Such a single 'external' front resistor, however, has to withstand for a short time the full rated voltage and therefore is inconveniently long or may occupy much space. This disadvantage can be avoided if either a part of this resistance is distributed or if it is completely distributed within the generator. Such an arrangement is illustrated in Fig. 2.30, in which in addition the series connection of the capacitors C'_1 and gaps (as proposed originally by Goodlet[38]) is changed to an equivalent arrangement for which the polarity of the output voltage is the same as the charging voltage. The charging resistors R' are always large compared with the distributed resistors R'_1 and R'_2, and R'_2 is made as small as is necessary to give the required time to halve-value T_2. Adding the external front resistor R''_1 helps to damp oscillations otherwise

mywbut.com

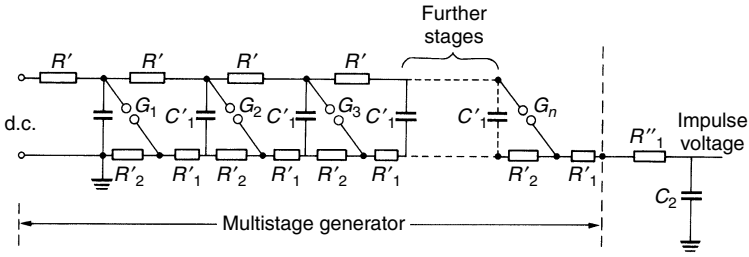


Figure 2.30 *Multistage impulse generator with distributed discharge and front resistors. R'_2: discharge resistors. R'_1: internal front resistors. R''_1: external front resistor*

excited by the inductance and capacitance of the external leads between the generator and the load, if these leads are long. It may be readily seen that this circuit can be reduced to the single-stage impulse generator circuit shown in Fig. 2.25(b). If the generator has fired, the total discharge capacitance C_1 may be calculated as

$$\frac{1}{C_1} = \sum^{n} \frac{1}{C'_1};$$

the effective front resistance R_1 as

$$R_1 = R''_1 + \sum^{n} R'_1;$$

and the effective discharge resistance R_2 – neglecting the charging resistances R' – as

$$R_2 = nR'_2 = \sum^{n} R'_2;$$

where n is the number of stages.

The consistent firing of such circuits could be explained as for the generator of Fig. 2.29. For both generator circuits, the firing is aggravated if the resistances R'_2 have relatively low values. According to eqns (2.22) and (2.39) such low values appear with generators of high energy content and/or short times to half-value, T_2. Then the time constant for discharging the stray capacitances to ground C''' (Fig. 2.29) will be too low and accordingly the overvoltages for triggering the upper stages too short. By additional means providing high resistance values within the firing period, this disadvantage can be avoided.[39]

Special circuits for generating switching impulse voltages

The common impulse generator circuits discussed so far are well capable of producing standard switching impulses with adequate voltage efficiency η, if the circuit is well designed and the ratio C_2/C_1 is kept adequately small.

mywbut.com

Other methods, however, have taken advantage of utilizing testing transformers to step up the amplitudes from impulse voltages also. One such circuit is shown in Fig. 2.31.[2] An initially charged capacitor C_1 is discharged into the waveshaping circuit R_1, C_2 as well as into the l.v. winding of the transformer. The elements R_1 and C_2 or other suitable components, in the dotted rectangle, may be used to control the waveshape. The wave tail is not only controlled by the resistive voltage divider included, but also from the main inductance of the transformer equivalent circuit. The time to crest T_p is even without R_1, C_2 limited by the series inductance of the transformer, L_s, which forms a series resonant circuit in combination with C_1 and the load capacitance C_2'. Neglecting any losses within the circuit, the voltage across the test object would therefore start with a $(1 - \cos \omega t)$ function, and as $T_p \approx T/2 = \pi/f_r$, f_r being the resonance frequency, the time to crest is approximately

$$T_{\text{cr}} \cong \pi\sqrt{L_s C}$$

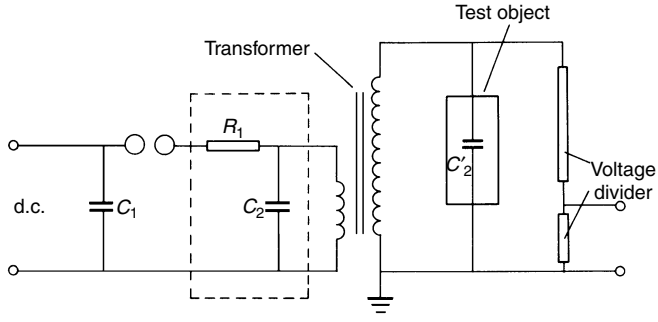


Figure 2.31 *Circuit for generation of switching impulses using a transformer*

where, neglecting transformer ratio,

$$C = \frac{C_1 C_2'}{C_1 + C_2'}.$$

In general, low values of T_p are difficult to achieve, as L_s is quite large and also the capacitance of the h.v. winding of the transformer contributes to the load C_2'. Further problems arise with transient oscillations within the transformer windings, mainly if cascaded testing transformers are used.[40]

The physical phenomena of disruptive discharges in long air gaps as well as in other insulating systems are often related to the front of switching impulses only. Therefore, with switching surges it is not always necessary to produce double-exponential waveshapes as recommended in Fig. 2.24. In

mywbut.com

fact, many investigations are sometimes made with unusual shapes of high voltages, and one can establish many circuits for mainly oscillating voltages, whose variety cannot be treated here. Only the common impulse voltage circuit with a strongly increased inductance will demonstrate this variety, as such circuits came into use for field testing of GIS.[41,42] The principle of such circuits is demonstrated in Figs 2.32(a) and (b). If the front resistor R_1 in Fig. 2.25(a) is replaced by a series inductance, the circuit of Fig. 2.32(a) results, which was first described for the generation of high switching impulse voltages up to 500 kV by Bellaschi and Rademacher.[43] A typical waveshape of the output voltage is also included; it may easily be calculated, since the circuit is a damped series resonant circuit only. The advantage of such a circuit is the nearly doubling of the output voltage, if $C_2 \ll C_1$, in comparison to the charging voltage V_0. Also a proper damping does not decrease the amplitude of the oscillation very much, and therefore the first increase of the voltage may be used as the front of a switching impulse. This fundamental circuit can be applied to multistage impulse generators, in which the front resistors are replaced by h.t. chokes.[42]

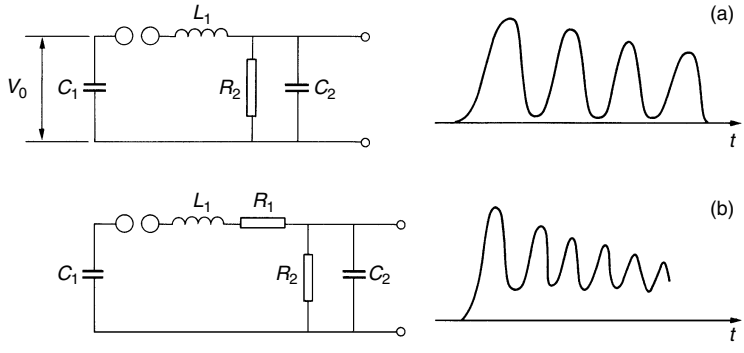


Figure 2.32 *Circuits for the generation of oscillating switching impulses*

A modular design of such generators offers the opportunity for easy transportation and erection on field site.

The second circuit of Fig. 2.32 uses an additional resistor R_1 in series to L_1, and is therefore simply a pure impulse voltage circuit with a high inductance within the discharge circuit. Therefore, unidirectional damped oscillations are produced. Also this circuit can be used for high voltages, as originally shown by Kojema and Tanaka.[44]

2.3.2 Operation, design and construction of impulse generators

Although the main aim of this book is not concerned with detailed information about the design and construction of h.v. equipment, some additional remarks

mywbut.com

are necessary for a better understanding of the problems involved with the operation and use of impulse generators. The advice given within this chapter is mainly related to section 2.3.1 and concerns multistage generators.

Every generator needs a d.c. power supply to charge the discharge capacitance C_1. This supply may simply consist of an h.t. transformer and rectifiers providing unidirectional currents, as the voltage smoothing is made by C_1. The d.c. supply should primarily act as a current source, so that the charging time can be controlled. The charging times should not be shorter than 5 to 10 sec, as every voltage application to an object under test may lead to prestressing effects within the insulation, influencing the withstand or breakdown strength. Much longer charging times or time intervals between successive voltage applications may be necessary, depending upon the material tested. For the rough-controlled charging, the d.c. supply is usually only voltage controlled by a voltage regulator at the primary of the h.t. transformer. Manufacturers nowadays provide thyristor-controlled charging supplies with current-limiting output. By this method, a programmed charging of generators is possible to reach equal charging times for all levels of impulse voltages.

The layout of the construction of multistage impulse generators is largely governed by the type of capacitors involved. Oil-paper-insulated capacitors of low inductance and high capability for fast discharging are in common use; mineral oil is often replaced by special fluids, providing higher permittivity to increase the capacitance per volume.

For earlier constructions predominantly capacitor units have been used, having the dielectric assembled in an insulating cylinder of porcelain or varnished paper with plane metal end-plates. This construction provided the obvious advantage that the stages of capacitors could be built up in the vertical columns, each stage being separated from the adjacent one by supports of the same or similar form as the capacitor units without dielectric. Such a construction is illustrated by the generator shown in Fig. 2.33. The disadvantage relates to the difficult replacement of failing capacitor units, and therefore this originally preferred construction is not much used today. New designs prefer complete modular constructions with capacitor units within insulating cylinders or vessels, or within metal tanks and bushings. This design originated from improvements in the capacitor dielectrics, which could reduce the size of the capacitors significantly even for voltages up to 100 kV per unit or more. To improve the consistency in firing the spark gaps, especially in cases of large generators with many stages, the gaps are mounted inside a cylindrical housing in which the pressure can be controlled, and hence the gaps do not require adjusting. Such a construction is shown in Fig. 2.34 for a 20-stage, 4-MV, 200-kJ indoor generator. Besides such indoor constructions, many of the generators for very high impulse voltages are used under outdoor conditions for the direct testing of outdoor material and to avoid the use of too large laboratories. To eliminate the detrimental influence of weather conditions

mywbut.com

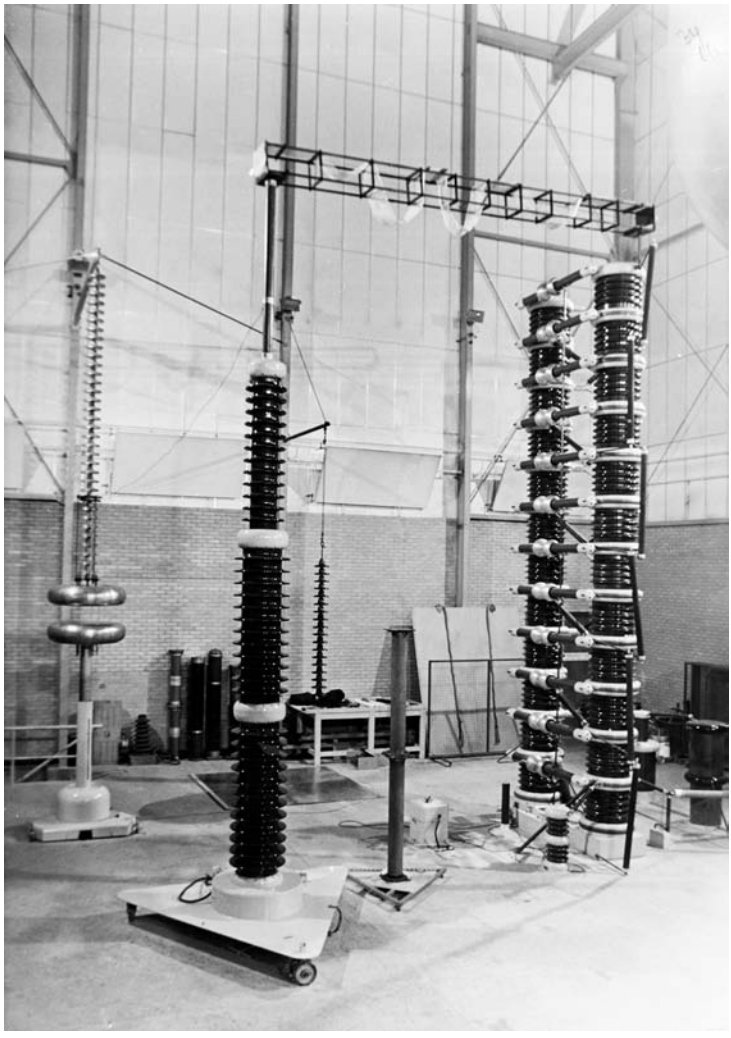


Figure 2.33 *2.4-MV impulse generator UMIST*

on electrical insulation as well as the mechanical influences (corrosion, etc.), most of these generators are housed in huge insulating cylinders providing for the full insulation of the output voltage and providing the opportunity to have the generator itself under air conditioning.

Besides the charging resistances R', all of the waveshaping resistors should be placed in such a way that they can easily be exchanged and replaced, as they must be changed often to ensure the waveshapes necessary.

mywbut.com



Figure 2.34 *Indoor impulse generator, 20-stage, 4-MV, 200-kJ, with encapsulated sphere gaps (courtesy of CEPEL, Rio de Janero, manufactured by Haefely)*

The resistors may be composed of wire, liquids or composite resistive materials. Although the high heat capacity involved with liquid and composite resistors would give preference to these resistor types, the instability of the resistance values is of big disadvantage. Therefore highly non-inductively wound wire resistors are best for the front and discharge resistors R_1 and

mywbut.com

R_2 of the circuits. Wavefront resistors are quite satisfactory if their L/R value is less than about 0.1 μsec.

The spark gaps are usually mounted on horizontal arms and the setting of the gaps is adjusted by a remotely controlled motor in conjunction with an indicator. This remark is, of course, related to gaps working in open air only. Sometimes encapsulated and pressurized gaps are used, for which the breakdown voltage is controlled by the gas pressure. The use of proper gas mixtures gives good switching performance.(45)

Each generator should have a device to earth the capacitors when it is not in operation. Due to relaxation phenomena, d.c.-operated capacitors can build up high voltages after a short-time short-circuit.

All leads and electrodes within the generator should be dimensioned properly to avoid too heavy corona discharges during the charging period. During the short time of discharge and therefore impulse generation, partial discharges cannot be prevented. A complete immersion of the generators in improved insulation materials, as mineral-oil or high-pressure gases, could reduce the size effectively; such solutions, however, are only used for special purposes.(46,47)

Finally, some explanations refer to the tripping and synchronization of the operation of impulse generators. The simple method of tripping the generators by non-triggered sphere gaps suffers from the disadvantage that the exact instant of firing is not predictable. Furthermore, the presence of unavoidable dust can cause irregular operation of multistage generators due to the following main reason: dust particles are likely to be attracted to the spheres stressed with d.c. voltages during charging, and the breakdown voltage can strongly be reduced by these particles.(48) If dust is randomly deposited on the lowest gap (G_1 in Fig. 2.29 or 2.30), the dispersion of the d.c. breakdown voltage of this gap increases and thus the output voltage will not be stable. To overcome this irregular firing of generators, which even with triggered gaps may occur, a protection against dust may be provided. As separate enclosures of the gaps with any insulating material prevents any ultraviolet illumination from reaching the other gaps, only a common enclosure of all gaps is satisfactory. Early investigations demonstrating those effects have been described by Edwards *et al.*(31) The common enclosure of all gaps provides, today, a reliable method to ensure stable tripping (see Fig. 2.34).

A stable self-tripping by a fast mechanical closure of the first gap is a simple means to avoid self-firing due to dust particles; however, this method cannot be used to synchronize the impulse voltage with other events within a very short time interval of a microsecond or less. The early need for synchronization arose from the necessity to initiate the time sweep of oscilloscopes used for the voltage recording. Later on, analogue impulse oscilloscopes have been manufactured with built-in time delays, so that a pre-trigger may not be necessary. Today, triggered firing of impulse generators would not be even

mywbut.com

required as transient recorders are available (see Chapter 3) which replace the analogue impulse oscilloscopes and which provide a continuous pre-trigger system. However, as such recorders may still not yet be in common use and since controlled or triggered switching of high voltages has so many applications in different fields, a brief review of controlled switching devices will be presented.

There are many factors and properties which have to be considered if controlled switching of voltages has to be achieved. The most essential factors include:

- the magnitude of the switched voltage (some kV up to MV),
- the magnitude of the control voltage or signal,
- the time delay between control signal and final stage of the switching,
- the jitter of the time delay,
- the conductivity of the switch in open and closed position,
- the inductance of the switch,
- the magnitude of the current switched,
- the repetition or recurrence frequency, and finally,
- the number of switching operations admissible.

For voltages higher than about 10 kV no solid state electronic element is able to operate. Up to some 10 kV, different types of thyratrons may be used, especially those with heated cathode and hydrogen content. Special types of thyratrons may switch voltages up to 100 kV and currents up to 20 kA with time delays of about 10 μsec and very low jitter down to a few nanoseconds. These elements are expensive, however, and the application is aggravated by the energy supply for the heated cathode, if the cathode is at high potential. Thus, for voltages higher than 100 kV only spark gaps are nearly unlimited in application, if they are properly controlled.

The physical mechanism responsible for the very fast transition of the resistance value of a spark gap begins with the streamer breakdown of the insulating gas and finishes with the arc, which has unlimited current-carrying capabilities. The time-dependent resistance of a gap may be calculated from the well-known 'spark laws' due to Toepler, Rompe-Weizel or Braginskii.[49] Investigations show that the oldest law associated with Toepler may conveniently be used for the computation of this time-dependent resistance, $R(t)$. If $i(t)$ is the current flowing in the gap, this resistance is given as

$$R(t) = \frac{k_T d}{\int_0^t i(t)\,\mathrm{d}t}$$

where d is the gap distance and k_T the 'Toepler spark constant'. The integration may be started ($t = 0$) by a finite, not too small, current, due to the early beginning of the spark formation. The values of k_T are not real constants; they

mywbut.com

are slightly dependent upon the gas involved and the field strength within the gap before breakdown. For air, many measurements have yielded a value of $k_T \cong 0.5 \times 10^{-4} \pm 20$ per cent Vs/cm. The above relationship may be applied to a discharge circuit consisting of a discharge capacitor C in series with a resistance R and a homogeneous spark gap to calculate the current $i(t)$ and the time-dependent voltage drop across the gap. If then a time to breakdown T_b is defined as the time from the 90 to the 10 per cent instant values of the decreasing voltage, for $C \gtrsim 2$ nF, $R \gtrsim 100\,\Omega$ one may derive the dependency

$$T_b \cong 13 \times 10^6 \frac{k_T}{E},$$

where T_b is in ns, k_T in Vs/cm and E in kV/cm. Thus for short switching times high field strength E before breakdown is necessary. Such high values can be achieved by pressurizing the gap, as the breakdown strength will increase about proportionally with the gas pressure (see Chapter 5, section 5.5). Also in air at atmospheric pressure switching times of about 20 ns will be reached for voltages up to some 100 kV.

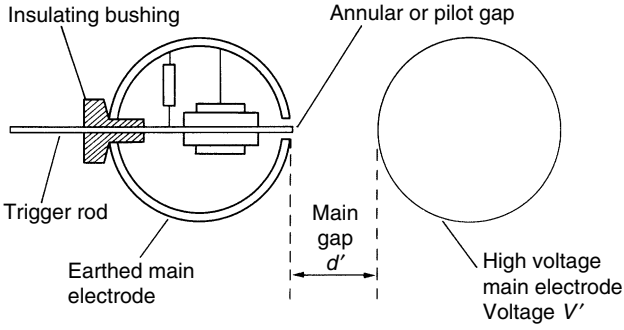


Figure 2.35 *The Trigatron spark gap*

The development of triggered and therefore controlled spark gaps cannot be discussed in detail. Only the principle will be considered using the arrangement displayed in Fig. 2.35, which provides good operating characteristics. This arrangement, known as 'Trigatron', consists essentially of a three-electrode gap. The main electrodes – indicated as h.v. and earthed electrodes – may consist of spheres, hemispheres or other nearly homogeneous electrode configurations. A small hole is drilled into the earthed electrode into which a metal rod projects. The annular gap between the rod and the surrounding sphere is typically about 1 mm. The metal rod or trigger electrode forms the third electrode, being essentially at the same potential as the drilled electrode, as it is connected to it through a high resistance, so that the control or tripping pulse

mywbut.com

can be applied between these two electrodes. For this special arrangement, a glass tube is fitted across the rod and is surrounded by a metal foil connected to the potential of the main electrode. The function of this tube is to promote corona discharges around the rod as this causes photoionization in the pilot gap, if a tripping impulse is applied to the rod. Due to this photoionization primary electrons are available in the annular gap which start the breakdown without appreciable time delay. The glass tube (or a tube of different solid insulation material, such as epoxy resin) may also fill the annular gap, so that the rod as well as the tube with its face is flush with the outside surface of the sphere. Thus a surface discharge is caused by the tripping pulse.

If a voltage V stresses the main gap, which is lower than the peak voltage at which self-firing occurs, this main gap will break down at a voltage even appreciably lower than the self-firing voltage V_s, if a tripping pulse is applied. The Trigatron requires a pulse of some kilovolts, typically $\leq 10\,\text{kV}$, and the tripping pulse should have a steep front with steepness $\gtrsim 0.5\,\text{kV/nsec}$ to keep the jitter of the breakdown as small as possible. The first essential operating characteristic refers to the voltage operating limits, at which a steady operation or switching is possible. Such a characteristic is sketched in Fig. 2.36, where the operating voltage V, the voltage across the main gap, is shown in dependency of the main gap distance. The upper operation limit is identical with the self-firing voltage as defined earlier; the lower operating limit is that at which still a steady operation or breakdown is obtained with a predetermined jitter, for instance $\leq 100\,\text{ns}$, or time delay. Such a characteristic is clearly dependent

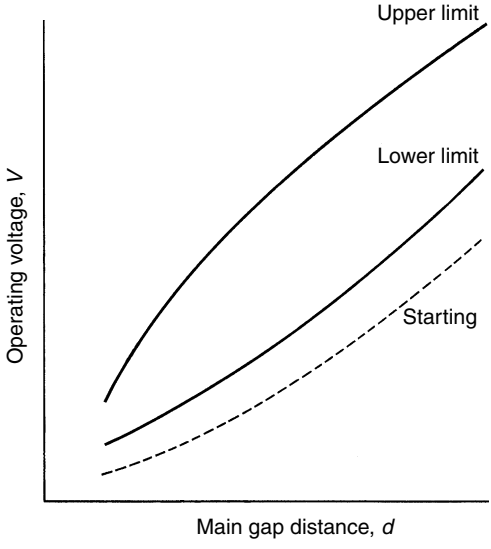


Figure 2.36 *Sketch of an operating characteristic of a Trigatron*

mywbut.com

upon the detailed construction of the Trigatron. These characteristics are also polarity sensitive, mainly if the field distribution within the gap is not very homogeneous; the polarity sensitivity refers also to the polarity of the tripping pulse, which should always be of opposite polarity of the main voltage which had to be switched.

The physical mechanism which causes the main gap to break down is fundamentally understood, although it might be quite complex in detail. Indeed, it is recognized today that two types of mechanism are active. For small spacings d and a given tripping voltage V, the breakdown may directly be initiated by the distortion and enhancement of the electrical field between trigger electrode and the opposite main electrode, leading to a direct breakdown between these two electrodes. The arc then commutates from the larger electrode to the drilled electrode for the main current. The second type of breakdown takes place for larger gap distances. The trigger pulse causes a breakdown of the annular or pilot gap, and the large amount of charge carriers of all types available after sparking will initiate the breakdown of the main gap.